JJC *Jordan Journal of Chemistry* Vol. 11 No.2, 2016, pp. 128-145

Sorption of 4-Nitroaniline on Activated Kaolinitic Clay and *Jatropha curcas* Activated Carbon in Aqueous Solution

Samsudeen O. Azeez[a*] and Folahan A. Adekola[b]

[a]*Chemistry Unit, Department of Chemical, Geological and Physical Sciences, Kwara State University Malete, P.M.B. 1530, Ilorin, Nigeria.*
[b]*Department of Industrial Chemistry, University of Ilorin, P.M.B 1515, Ilorin 240003, Nigeria.*

Received on April 19, 2016 **Accepted on** June 19, 2016

Abstract

A comparative study was carried out of the adsorption of 4-nitroaniline (4-NA) on activated kaolinitic clay and Jatropha curcas activated carbon. The kaolinitic clay and Jatropha curcas samples were activated with 1 M HNO_3 and 0.5 M NaOH, respectively, and were characterized using XRF, XRD, BET, SEM and FTIR techniques. The effects of various experimental parameters, such as the initial 4-nitroaniline (4-NA) concentration, temperature, pH, contact time and adsorbent dosage on the adsorption process were investigated. The results obtained showed that Jatropha curcas activated carbon exhibited a better performance for the removal of 4-nitroaniline (4-NA) from aqueous media. The adsorption process was found to obey pseudo-second order kinetics and equilibrium data were best fitted with the Freundlich isotherm. The adsorption process was found to be independent of temperature.

Keywords: Activated kaolinitic clay; Adsorption isotherm; Jatropha curcas activated carbon; Kinetics; Thermodynamics; 4-nitroaniline.

Introduction

4-nitroaniline (4-NA) is an important compound industrially used as a precursor in the manufacture of several organic compounds and materials such as p-phenylenediamine, azo dyes, antioxidants, fuel additives, corrosion inhibitors, pesticides, antiseptic agents, medicines for poultry as well as in the synthesis of pharmaceuticals.[1-2] Because of its high solubility in water, 4-NA imparts taste and odour on water even at parts per billion levels. It is also extremely harmful to aquatic life and human health due to its hematoxicity, splenotoxicity and nephrotoxicity, meaning that they damage all kind of cells.[3] Moreover, the presence of a nitro group in the aromatic ring of 4-NA makes it resistant to chemical and biological oxidative degradation, while its anaerobic degradation produces nitroso and hydroxylamines compounds that are carcinogenic.[4] Hence, there is a need to remove 4-NA from waste effluents generated from these industries before being discharged into rivers or public sewage networks. Until now, various treatment technologies have been

* Corresponding author: e-mail: samsudeen.azeez@kwasu.edu.ng

proposed for the removal of 4-NA and other organic contaminants from wastewaters; these include advanced oxidation processes,[5-6] solvent extraction[7] and biodegradation,[8] electrochemical oxidation[9-10] and biochemical abatement.[11] Problems associated with the above mentioned methods include the high cost, low efficiency and the generation of toxic and secondary products.[12] Therefore, new cost-effective technologies for the removal of 4-NA are crucial. Adsorption has been chosen as one of the most widely acceptable effective techniques to remove 4-NA and other organic pollutants at higher concentration due to its relatively simple design, cost effectiveness, ease of operation and simple adsorbent regeneration.[13-14] A lot of adsorbents have been reported by researchers for the purpose of wastewater treatment and remediation. Examples include the adsorption of p-nitroaniline from aqueous solution onto activated carbon fibre prepared from cotton stalk[15] or onto activated carbon prepared from treated camphor wood.[16] The adsorption of phenol on natural clay[17] as well as onto activated phosphate[18] was also investigated. The removal of phenol from aqueous solution by activated carbon prepared from agricultural waste materials was studied[19] and the kinetics and thermodynamics of 4-nitrophenol adsorption on fiber-based activated carbon prepared from coconut husks was reported.[20] Consequently, as a result of growing interest in the use of low cost adsorbents for wastewater treatment and remediation, it becomes imperative to continue the research into the use of abundant minerals, such as kaolinite (largely abundant in Nigeria), as well as activated carbon prepared from a non-edible agricultural waste, such as the seed shell of *Jatropha curcas*, for wastewater treatment processes.

Kaolinitic clay is a clay that is rich in kaolinite, also known as china clay.[21] It is a layered silicate mineral of the chemical composition $Al_2Si_2O_5(OH)_4$ with one tetrahedral sheet of silica linked through oxygen atoms to one octahedral sheet of alumina.[22] It has many uses due to its favourable properties such as natural whiteness, fine particle size, non-abrasiveness and chemical stability. It is used as filler in the production of rubber, plastics and pigments as well as in the production of synthetic zeolites and as such, as an adsorbent in drugs.[23] *Jatropha curcas* is one of the species of the flowering plants in the genus *Jatropha* in spurge family, Euphorbiaceae, native to the American tropics, most likely Mexico and Central America.[24] It is a semi-evergreen shrub or small tree rather resistant to a high degree of aridity, which allows it to be grown in deserts. The seeds contain 27-40% oil that could be processed to produce a high-quality biodiesel fuel, usable in a standard diesel engine.[25, 26]

The prime objective of this study was to investigate the efficiency of activated kaolinitic clay (AKC) and Jatropha activated carbon (JAC) in the removal of 4-NA from aqueous solution. The effects of initial 4-NA concentration, pH, contact time, adsorbent dosage and temperature on the adsorption capacity were investigated. Kinetic and

thermodynamic models were used to fit the experimental data and deduce the corresponding parameters.

Materials and Methods

Reagents

The reagents and chemicals used in this work were of analytical grade: 4-nitroaniline (Sigma-Aldrich 99%), hydrochloric acid (37%, density 1.1 kg/cm^3, Riedel-deHaen), sodium hydroxide (BDH) and Nitric acid (98%, 1.51 g/cm^3, Sigma-Aldrich), were used without further purification.

The kaolinitic clay was sourced from Batagbon in Edu local Government Area of Kwara State, Nigeria. The *Jatropha curcas* fruit was collected from a private estate in Tanke area, Ilorin. The pericarp was cracked after air-drying in order to remove the seed; the seed coat was used for the preparation of activated carbon while the seed was saved for later use in biodiesel production.

Preparation of the adsorbents

Physical processing

The kaolin clay sample was ground with agate mortar and pestle, washed several times with deionised water then air dried for 24 h. The particle size fraction in the range -90+75 µm was separated using Tyler Standard sieves, then soaked in concentrated HCl solution for 4 h to eliminate impurities, washed several times with deionised water and finally oven-dried for 2 h.[18] The seed coat of *Jatropha curcas* was carbonised in a furnace at a temperature of 500 ^{o}C for 90 min. The carbonized product was then finely ground, and sieved with standard particle mesh into the particle size range -90+75µm.[19]

Chemical activation

100 g of the prepared kaolinitic clay fraction (-90+75 µm) was activated with 1 M nitric acid by adding 400 mL of the acid solution and stirring on a magnetic stirrer at a fixed rate of 500 rpm for 150 min at 90 °C. The sample was then filtered, washed several times with deionized water to neutral pH and dried at 105 °C to obtain activated kaolinitic clay (AKC).[17]

The sieved carbon prepared from *Jatropha curcas* seed coat was activated with 0.5 M NaOH; 50 g of the carbonised *Jatropha curcas* seed coats was impregnated in 200 mL of 0.5 M NaOH solution for 48 h. The sample was then filtered, washed with deionized water to neutral pH and oven-dried at 105 °C.[19]

Characterization of the adsorbents

The composition of the kaolinitic clay sample was determined using MINI PAL4 EDXRF Spectrometer. The crystal phases of kaolin were determined by means of X-ray diffraction (XRD) using a PANalytical X'Pert PRO MRD PW3040 model. The BET

surface area of both AKC and JAC was determined according to Brunauer, Emmet and Teller (BET) by N_2 adsorption at 77 K using Micromeritics ASAP 2020 V3.02H surface area and porosity analyzer. The surface morphology of the adsorbents was analysed using an ASPEX 3020 Scanning Electron Microscope (SEM). Fourier transform infrared absorption spectra were obtained using the potassium bromide (KBr) disc method and the spectra of the samples were recorded over the range 4000–400 cm^{-1} using a Shimadzu FTIR-8400S spectrometer.

Preparation of standard solution

A stock solution of 4-nitroaniline (4-NA) was prepared by dissolving 1.0 g of the adsorbate in ethanol in a 1000 mL volumetric flask. Various test solutions were then prepared by serial dilution of the stock solution with deionised water to the desired concentration (10, 20, 30, 40, 50, 100, 150 mg/L). The pH of the solutions was adjusted to the required value with 0.1 M HCl or 0.1 M NaOH.

Adsorption experiments

The adsorption experiments were carried out in batch mode. The experiment involves adding 0.20 g of AKC or 0.02 g of JAC to 20 mL of 4-NA solution of a given concentration (10, 20, 30, 40, 50, 100 or 150) mg/L). The mixture was agitated for 2 hr at 200 rpm at a temperature of 28±2 $^{\circ}$C. The pH of the solution, measured by a pH-meter, was adjusted using 0.1 M HCl or 0.1 M NaOH. The effect of various experimental parameters such as pH (2.0, 4.0, 6.0, 8.0, 10.0), contact time (5 to 1440 min), adsorbent dosage (0.10-0.50 g AKC and 0.01-0.05 g JAC) and temperature (30 $^{\circ}$C to 60 $^{\circ}$C) was studied. The solutions were then centrifuged at 10,000 rpm for 10 min and the supernatant solution was filtered and analysed for 4-NA using a Bechman Coulter DU 730 UV/Visible spectrophotometer at λ_{max} = 400 nm. The amounts of 4-NA adsorbed, q_e (mg/g), were calculated using equation 1:[20]

$$q_e = \frac{(C_0 - C_e)V}{W} \quad (1)$$

where C_0 and C_e are the initial and equilibrium concentrations of 4-NA (mg/L), V is the volume of the solution (L) and W is the mass of adsorbent used (g). The %Removal of 4-NA adsorbed was then calculated using equation 2:[20]

$$\%\, Removal = \frac{(C_0 - C_e)}{C_0} \times 100 \quad (2)$$

All experiments were performed in triplicate to ensure the reproducibility of the results; the mean of the measurements is reported.

Results and discussion

Composition of the kaolinitic clay

The composition of the kaolin sample is depicted in Table 1 where it can be seen that the major constituents of the clay are Al_2O_3 (43.3%) and SiO_2 (52.0%). High

grade Kaolin samples have been reported to contain Al_2O_3 (alumina) in the range (33 – 42%) [27].

Table 1: Chemical composition of kaolinitic clay sample as determined by XRF.

Compounds	Al_2O_3	SiO_2	K_2O	CaO	TiO_2	Fe_2O_3	MnO	Cr_2O_3	V_2O_5	Ag_2O
%	43.3	52.0	0.041	0.214	1.68	1.04	0.016	0.036	0.085	1.40

X-ray diffraction (XRD) of the kaolinitic clay

Figure 1 shows the x-ray diffraction pattern of AKC with intense peaks at 2θ values of 12.5°, 24.9° and 62.3° and with less intense peaks at 2θ values of 19.8°, 35.9°, 37.7° and 38.4° which, according to the JCPDS file no 01-078-1996[28] (green lines in the figure), are characteristic of kaolinite. The diffractogram shows also the diffraction peaks of quartz at 2θ values of 20.9°, 26.7° and 50.1° as identified by the JCPDS file no 01-079-1910[28] (red lines in the figure) for quartz.

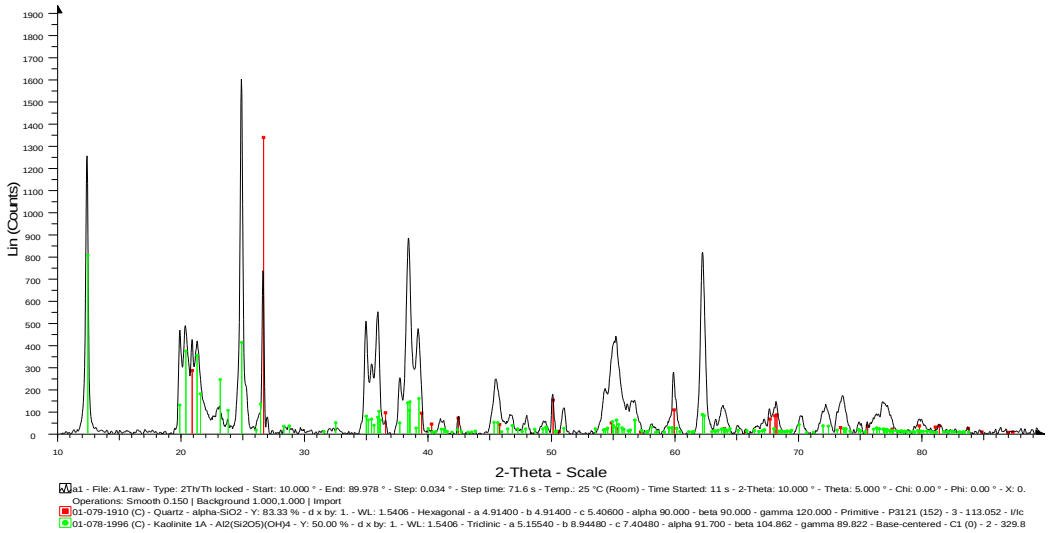


Figure 1: XRD patterns of AKC.

Surface area determination

The results of the surface area analysis of the adsorbents are tabulated in Table 2. In summary, the BET surface area and pore volume of JAC are higher than those of AKC while the pore size of AKC is greater than for JAC. According to the classification by the International Union of Pure and Applied Chemistry,[29] pores are classified as micropores (< 2 nm in diameter), mesopores (2-50 nm in diameter) and macropores (> 50 nm in diameter). Both AKC and JAC are composed correspondingly mainly of mesopores with surface area in the range of 20 to 50 m^2 per gram and pore size of

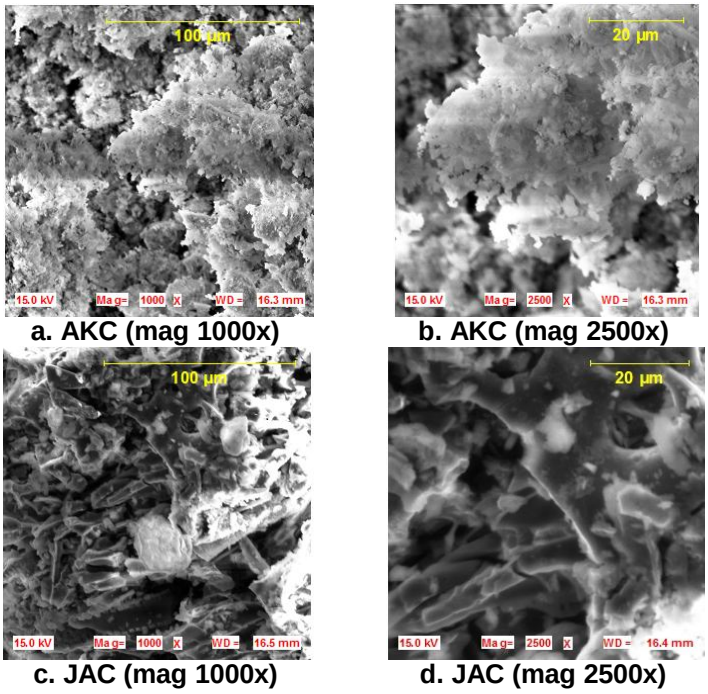
Table 2: BET results for AKC and JAC.

Adsorbents	**BET surface area (m^2/g)**	**Pore volume (cm^3/g)**	**Pore size (nm)**
AKC	20.60	0.0180	3.480
JAC	50.29	0.027	2.11

about 3.4 nm and 2.1 nm, respectively. The larger surface area and pore volume recorded for JAC with the pore size being in the mesopore region suggests that JAC might act as a better adsorbent in the uptake of 4-NA than AKC.

Scanning electron microscopy (SEM)

The SEM images of AKC and JAC are presented in Figure 2. The SEM images of AKC (Figure 2a-b) show the typical flake-like morphology of fine clay particles. The SEM micrographs of JAC (Figure 2c-d) indicated a more rough surface, the fragmented surface is due to carbonization and activation by chemical method.[30]



a. AKC (mag 1000x) **b. AKC (mag 2500x)**

c. JAC (mag 1000x) **d. JAC (mag 2500x)**

Figure 2: SEM images of the adsorbents

Fourier transform infra-red spectroscopy (FTIR)

The FTIR spectra of AKC and JAC before adsorption are presented in Figure 3(a-b). The FTIR spectrum of AKC (Figure 3a) reveals the characteristic bands of kaolinite appearing at 3696 cm^{-1}, 3655 cm^{-1}, 3620 cm^{-1} and 3586 cm^{-1} attributed to the stretching vibrations of the surface hydroxyl groups. The band observed at 3460 cm^{-1} and 3437 cm^{-1} were assigned to O-H stretching vibrations of adsorbed water. The band at 1101 cm^{-1} was attributed to the Si-O stretching. The band at 914 corresponds to the deformation of OH attached to Al, and bands at 792, 651 and 432 cm^{-1} were assigned to Si-O-Al and Si-O-Si bending vibrations. These functional groups are commonly found in silicate minerals such as kaolinite.[17, 31]

Figure 3b is the FTIR spectrum of JAC before adsorption. This figure shows a strong broad absorption peak at 3399 cm^{-1} representing the O-H stretching vibration of phenolic or acid groups but also of adsorbed water. The band recorded in the region of 1574 cm^{-1} corresponds to the C=C stretch in aromatic skeletal mode. In addition, there is a peak at 1373 cm^{-1} due to the C-O-H bending. Other important absorption bands

appear at 1038 cm^{-1} representing the C-O stretch of primary alcohol of lignin and at 1111 cm^{-1} attributed to C-O-C asymmetric stretch of ether groups of lignin.[32, 33]

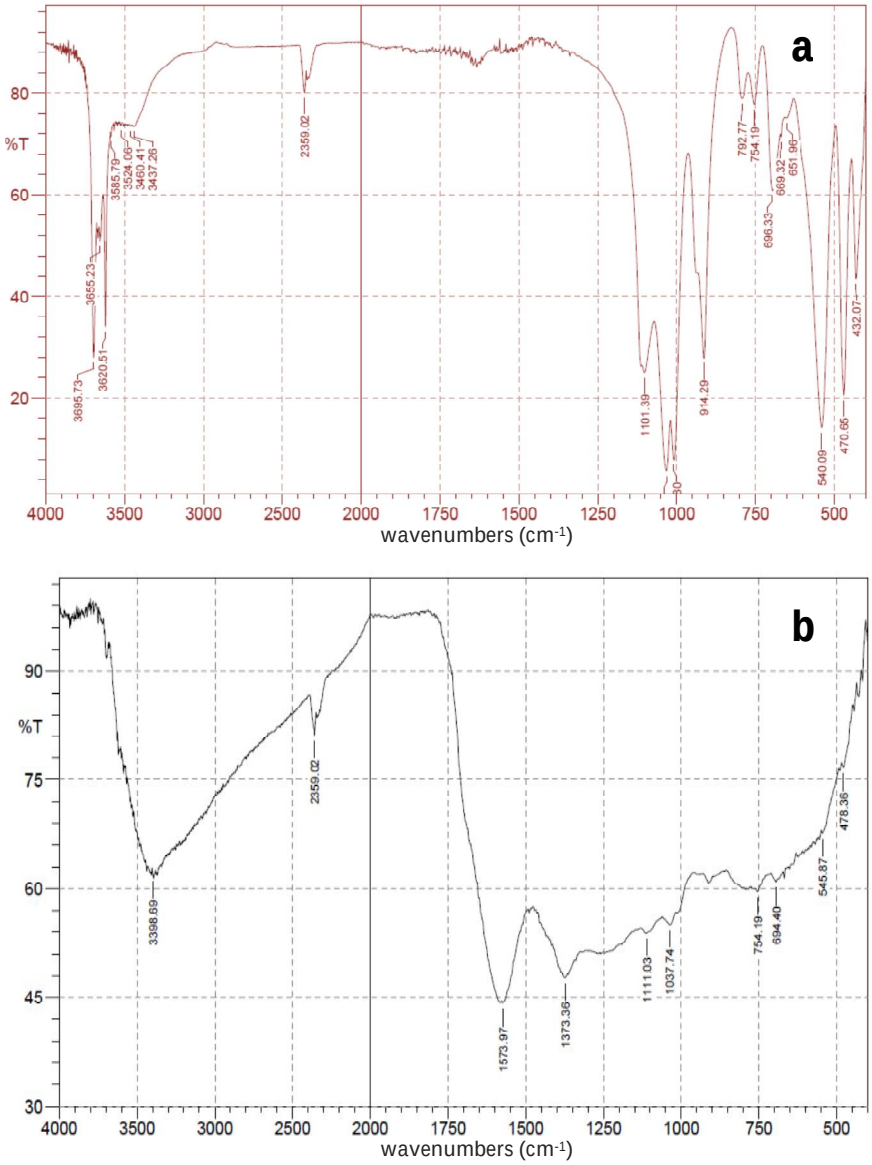


Figure 3: FTIR Spectra of AKC (a) and JAC (b).

Adsorption of 4-NA

Effect of initial concentration

Figure 4 illustrates that the amount of 4-NA adsorbed on JAC increases as the initial 4-NA concentration increases from 10 to 150 mg/L. On the other hand, the sorption of 4-NA onto AKC was practically negligible as there was no significant difference between the initial and final concentrations of 4-NA in solution. This shows that JAC is more effective in adsorbing 4-NA than AKC which can be attributed to the higher surface area and pore volume of JAC as well as to the different nature of the adsorbing surface.[20]

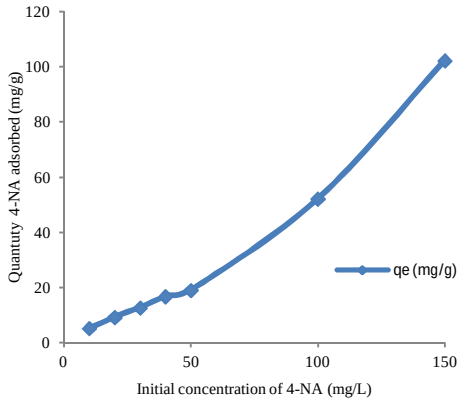


Figure 4: Effect of initial 4-NA concentration; w= 0.02 g, pH = 2, T = 28±2 ºC for 2 h at 200 rpm, (n=3, 0 ≤ % E ≤ 0.97).

Effect of pH

The pH of the solution is an important variable that affects the surface charge of the adsorbent and the degree of ionisation and speciation of the adsorbate species, which may lead to changes in the kinetic and equilibrium characteristics of the adsorption process.[20] The influence of pH on the removal of 4-NA by JAC is depicted in Figure 5 which shows that relatively higher adsorption was recorded at low pH, a behaviour that can be ascribed to the protonation of 4-NA at low pH values favouring thus the uptake of 4-NA. The higher uptake of 4-NA at pH = 2 could probably be due to the electrostatic attraction between the adsorbent surface and the lone pair electrons on the amino groups of 4-NA. This result is however in disagreement with literature reports. For the adsorption of p-nitroaniline from aqueous solutions onto activated carbon fiber prepared from cotton stalk, El-Shahat and Shehata report an optimum pH value of 7.[16] Kunquan et al. report also an optimum pH value of 7.6 for the adsorption of p-nitroaniline onto activated carbon prepared from treated camphor wood.[15] The pKa value of the conjugate ammonium species of 4-NA is 1 which means that it dissociates further at pH slightly greater than its pKa. Apparently, the adsorption decreases at pH > 2 due to the dissociation of the ammonium species. Another factor contributing for the observed behaviour could be the electrostatic repulsion between the negatively charged surface of the adsorbent and the lone electron pairs of 4-NA.[34]

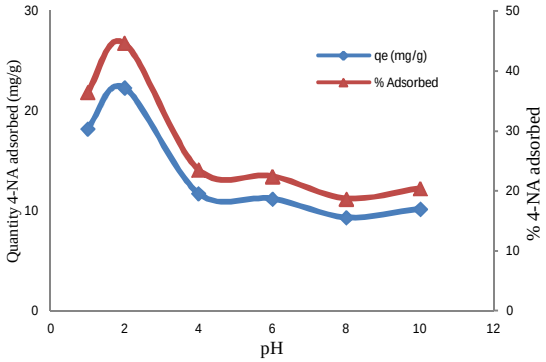


Figure 5: Effect of pH: Co = 50 mg/L, w = 0.02 g, T = 28±2 ºC for 2 h at 200 rpm, (n=3, 0 ≤ % E ≤ 0.33).

Effect of contact time

In order to find out the time needed to reach equilibrium, the interaction period for 4-NA on JAC was varied for an initial concentration of 50 mg/L from 5 to 1440 min and the percentage adsorbed was plotted versus the contact time as depicted in Figure 6. It can be observed that at the initial stage, the rate of adsorption was very fast as over 30% of 4-NA was adsorbed in the first 5 min. The rate of adsorption begins thereafter to decrease (over 40% in 30 min) until it finally reaches zero at equilibrium (plateau) after about 120 min with the amount adsorbed being 29.3 mg/g (removal=58.54%). The sharp rise in adsorption at the initial stage is an indication that at the beginning there are several available sites to be occupied, their number decreases with time until eventually a plateau is reached indicating the establishment of adsorption-desorption equilibrium.[35, 36]

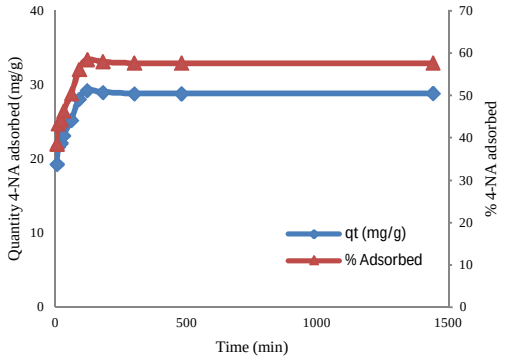


Figure 6: Effect of contact time: Co = 50 mg/L, w = 0.02 g, pH = 2, T = 28±2 ºC for 5 – 1440 min at 200 rpm, (n=3, 0 ≤ % E ≤ 0.98).

Effect of adsorbent dosage

The determination of optimum dosage is essential for the optimisation of the adsorption process. It is evident from Figure 7 that with increased JAC dosage for a fixed initial 4-NA concentration, the percentage adsorbed increased rapidly. The removal of 4-NA increased from 30.6% with 0.01 g JAC to 89.2% with 0.05 g JAC. The quantity of 4-NA adsorbed was initially in the range 0.01- 0.02 g JAC constant before starting to decrease significantly for dosages between 0.03-0.05 g JAC. The rapid removal of 4-NA observed at the early stage of the experiment is attributed to the availability of a large number of free adsorption sites on the adsorbent surface.[37] As time goes by, the number of free adsorption sites gradually decreases as well as the concentration of the 4-NA in solution leading to reduced sorption probabilities.

Effect of temperature

The effect of temperature on the adsorption of 4-NA by JAC was examined in the range of 30-60 ºC; the experimental results are presented in Figure 8. The quantity adsorbed was determined as 22.41, 23.88, 24.06 and 21.82 mg/g at 30, 40, 50 and 60 °C respectively as shown in figure 8 and it can be seen that the quantity of 4-NA adsorbed by JAC is practically independent of temperature as there is no significant

difference in the quantity of 4-NA adsorbed over the temperature range studied, suggesting zero heat of adsorption.

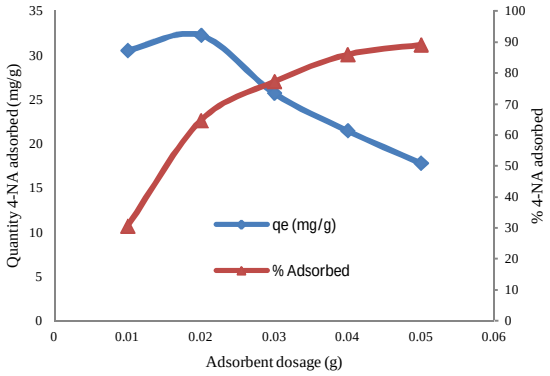


Figure 7: Effect of adsorbent dosage: Co = 50 mg/L, pH = 2, T = 28±2 ºC for 2 h at 200 rpm, (n=3, 0 ≤ % E ≤ 0.02).

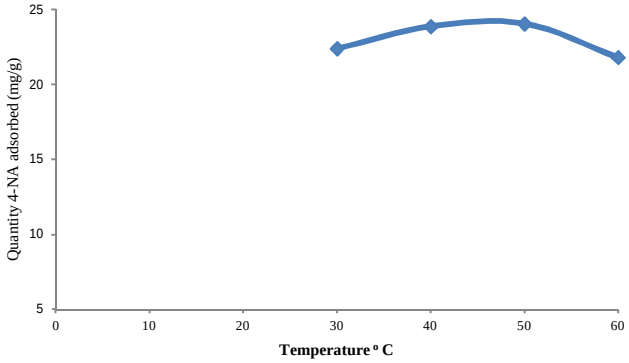


Figure 8: Effect of temperature: Co = 50 mg/L, w = 0.02 g, pH = 2, for 2 h at 200 rpm, (n=3, 0 ≤ % E ≤ 0.03).

Adsorption isotherm

Adsorption isotherms are basically important to describe how solutes interact with adsorbents and are critical in optimizing the adsorption process. The equilibrium adsorption data of 4-NA on JAC was analysed using the Langmuir, Freundlich, Temkin and Dubinin-Radushkevich (D-R) isotherms. The closer the value of the regression coefficient (R^2) to unity, the better is the agreement of the experimental data with the model isotherm. The Langmuir isotherm model is valid for monolayer adsorption on a surface containing a finite number of identical sites, assuming a homogeneous distribution of sorption energies. A linear form of the Langmuir isotherm is represented in equation 3. The dimensionless equilibrium parameter (R_L) expressed by Equation 4 confirms the favourability of the adsorption process. The adsorption process is said to be favourable if R_L value falls between 0 and 1 ($0 < R_L < 1$), linear when R_L=1, irreversible when R_L = 0 and unfavourable when $R_L > 1$.The heterogeneity of the surface is better described by the Freundlich isotherm as presented in Equation 5. The Temkin model assumes that heat of adsorption (function of temperature) decreases linearly with coverage as represented in equation 6.[20] The Dubinin-Radushkevich (D-

R) isotherm is generally applied to multi-layer adsorption and expresses the adsorption mechanism with a Gaussian energy distribution onto a heterogeneous surface. The model has been found to successfully fit the data of high solute activities and intermediate range of concentrations.[38] The linearised equation is expressed in equation 7.

$$\frac{C_e}{q_e} = \frac{1}{Q_{0\,K_L}} + \frac{1}{Q_0}\,C_e \tag{3}$$

$$R_L = \frac{1}{1 + K_L C_o} \tag{4}$$

$$\log q_e = \log k_f + \frac{1}{n}\log C_e \tag{5}$$

$$q_e = \frac{RT}{b_T} lnA_T + \frac{RT}{b_T} lnC_e \tag{6}$$

$$\ln q_e = \ln q_D - B_D\,\mathcal{E}^2 \tag{7}$$

where c_e is the equilibrium concentration of the adsorbate (mg/L), q_e the amount of adsorbate adsorbed per unit mass of adsorbate (mg/g), Q_o and K_L are the adsorption capacity and the Langmuir equilibrium constant of adsorption, respectively. K_F and n are the Freundlich constants, n is an indication of how favourable the adsorption process is and K_F reflects the adsorption strength. A_T is the Temkin equilibrium constant (L/g), b_T is the Temkin constant related to the heat of sorption (J/mol), R is the universal gas constant (8.314 J/mol/K), and T is the absolute temperature. q_D is the theoretical adsorption capacity (mg/g), B_D is a constant related to the adsorption energy E (mol^2/J^2) and ε is the Polanyi potential related to the equilibrium concentration as represented by equation 7a and 7b respectively:

$$E = \frac{1}{\sqrt{2B_D}} \tag{7a}$$

$$\mathcal{E} = RT \ln\,[1 + \frac{1}{C_e}] \tag{7b}$$

Figure 9 represents the plots of the Langmuir, Freundlich, Temkin, and Dubinin-Radushkevich (D-R) isotherms and Table 3 lists all their parameters. The high correlation coefficient for the Freundlich isotherm suggests that it describes adequately the adsorption of 4-NA onto JAC; the other three models show lower R^2 values. The value of the Freundlich constant n (1.43) is greater than 1 suggesting that the adsorption process is favourable. The constant K_f, an indication of the adsorption affinity between 4-NA and JAC, has a value 1.79 (mg/g). The Temkin constants A_T, B and b_T are as listed in Table 3; the low value of B= 7.436 J/mol indicates a small heat of sorption. The Langmuir model with a correlation value of 0.95 gives a maximum monolayer adsorption capacity (Q_o) of 38.76 mg/g. The adsorption process is favourable since R_L falls between 0 and 1. The experimental data do not fit well into the D-R model.

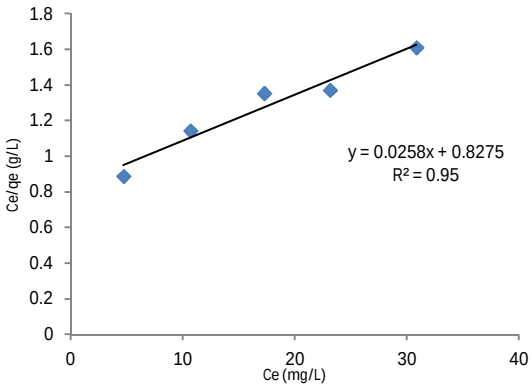


Figure 9a: Langmuir Isotherm for the sorption of 4-NA onto JAC.

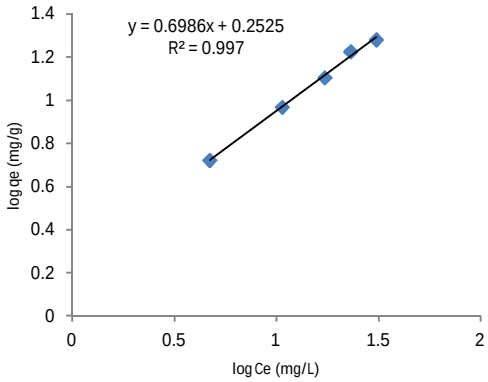


Figure 9b: Freundlich Isotherm plot for the sorption of 4-NA onto JAC.

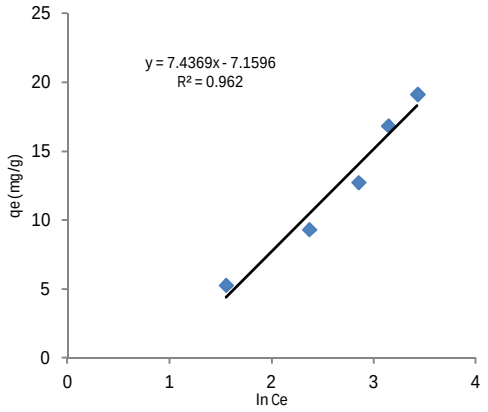


Figure 9c: Temkin Isotherm plot for the sorption of 4-NA onto JAC.

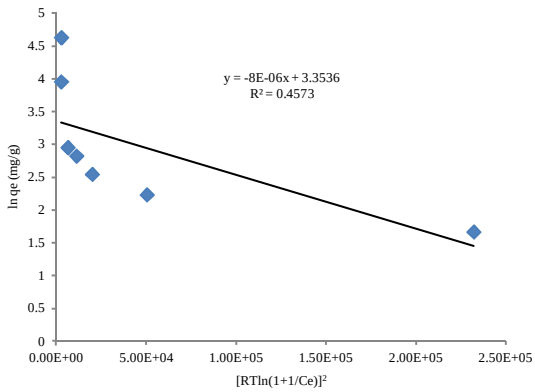


Figure 9d: Dubinin-Radushkevich Isotherm plot for the sorption of 4-NA onto JAC.

Table 3: Isotherm parameters for the sorption of 4-NA onto JAC.

Isotherm	Parameters	Values
Dubinin-Radushkevich	B_D (mol^2/J^2)	8.0×10^{-6}
	q_D (mg/g)	28.60
	E (kJ/mol)	0.250
	R^2	0.457
Freundlich	K_f (mg/g)	1.97
	n	1.43
	R^2	0.997
Langmuir	Q_o (mg/g)	38.76
	K_L ($L.mg^{-1}$)	0.031
	R_L	0.39
	R^2	0.95
Temkin	B	7.44
	A_T (Lg^{-1})	1.70
	b ($Jmol^{-1}$)	333.2
	R^2	0.966

Kinetic models

The kinetics of 4-NA adsorption onto JAC was studied. Four types of kinetic models were considered: pseudo-first-order, pseudo-second order, Elovich and Intra-particle diffusion models.

The Pseudo-first-order rate expression (Lagergren, 1898) is given as

$$\ln(q_e - q_t) = \ln q_{e,cal} - K_1 t \quad (8)$$

The pseudo-second-order kinetic model equation is given as

$$\frac{t}{q_t} = \frac{1}{K_2 {q_{e,cal}}^2} + \frac{t}{q_{e,cal}} \quad (9)$$

The Elovich equation is expressed as

$$q_t = \frac{1}{\alpha}\ln(\alpha\beta) + \frac{1}{\alpha}\ln t \quad (10)$$

The intra-particle diffusion equation is expressed as

$$q_t = K_{diff}\sqrt{t} + C \quad (11)$$

where, q_e (mg/g) and q_t (mg/g) are the amounts of 4-NA adsorbed at equilibrium and at any time t (min), respectively. k_1 (min^{-1}), k_2 (g/mg min) and K_{diff} (mg/g $min^{1/2}$) are the rate constants of the pseudo-first-order, pseudo-second-order and the intra-particle diffusion models, respectively. α is the initial adsorption rate (mg/g min) and β is the desorption constant (g/mg). C is another constant that gives information about the thickness of the boundary layer.[20, 39] The pseudo-second order plot of t/q_t against t given in figure 10b shows that the plot has a good linearity and yielded a second order rate constant of 5.39×10^{-3} g mg^{-1} min^{-1} with regression coefficient (R^2) of 0.998. There is a close agreement between the calculated q_e value (30.0 mg/g) and the experimental q_e value (29.3 mg/g).[15, 16] Hence, this model describes adequately the adsorption kinetics of 4-NA onto JAC. The pseudo-first order and Elovich kinetic models have lower regression values of 0.892 and 0.937, respectively, as shown in Table 4 and figures 10a and 10c.

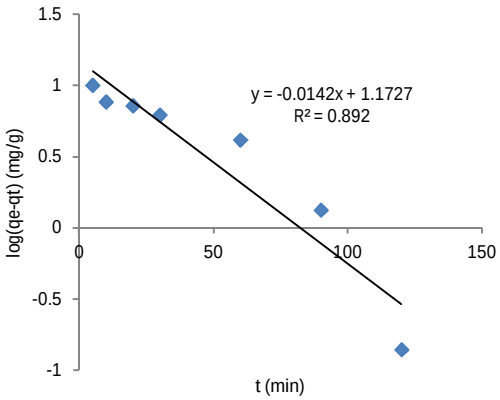


Figure 10a: Pseudo-first order kinetic model for 4-NA adsorption onto JAC.

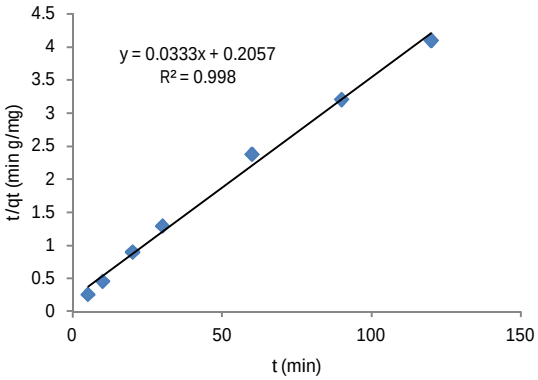


Figure 10b: Pseudo-second order kinetic model for 4-NA adsorption onto JAC.

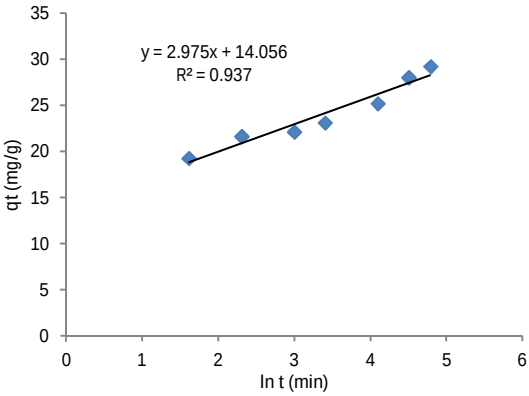


Figure 10c: Elovich kinetic model for 4-NA adsorption onto JAC.

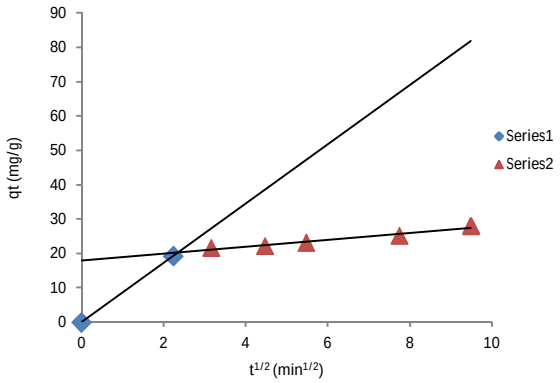


Figure 10d: Intra-particle diffusion model for 4-NA adsorption onto JAC.

Table 4: Parameters and correlation coefficients of the kinetic models for 4-NA adsorption onto JAC.

Kinetic models	Parameters	Values
Pseudo-first order model	K_1 (min^{-1})	0.033
	$Q_{e,\,cal}$ (mg/g)	3.23
	R^2	0.892
Pseudo-second order model	K_2 (g/mg/min)	5.39x10^{-3}
	$Q_{e,\,cal}$ (mg/g)	30.03
	R^2	0.998
Elovich	α	0.336
	β	334.8
	R^2	0.937
Intra-particle diffusion	Line 1	Line 2
K_{diff} (mg g^{-1} min$^{1/2}$)	8.63	1.01
C	0	17.92
R^2	1.00	0.96

The intra-particle diffusion constants K_{diff} and C values evaluated from Figure 10d and are presented in Table 4. A multi-linear plot was obtained for the intra-particle diffusion model and is of two stages. The first stage is the sharply rising part which depicts adsorption due to boundary layer diffusion while the second stage involves the intra-particle diffusion of adsorbate until equilibrium was attained. Obviously, intra-particle diffusion has plays a smaller role in the adsorption process compared with surface diffusion. The deviation of the plot from the origin indicates that pore diffusion was not the sole rate-controlling step.[39]

Thermodynamic parameters

The thermodynamic parameters provide information about the feasibility of the adsorption process as well as the stability of the adsorbed phase.[40] The thermodynamic parameters such as change in enthalpy (ΔH^o) and entropy (ΔS^o) can be estimated from the slopes and intercepts of the linear plot (Figure 11) of equation 13, while the change in free energy (ΔG^o) can be calculated from the obtained values of ΔH^o and ΔS^o using equation 14.[41]

$$\Delta G = -RTInK \quad (12)$$

$$lnK_c = \frac{\Delta S}{R} - \frac{\Delta H}{RT} \quad (13)$$

$$K_c = \frac{q_e}{C_e(q_0 - q_e)}$$

$$\Delta G^o = \Delta H^o - T\Delta S^o \quad (14)$$

where ΔG^o, ΔH^o and ΔS^o are the standard changes in free energy (kJ/mol), enthalpy (kJ/mol) and entropy (kJ/mol.K), respectively. R is the universal gas constant and T is the absolute temperature (K) at which adsorption was conducted.

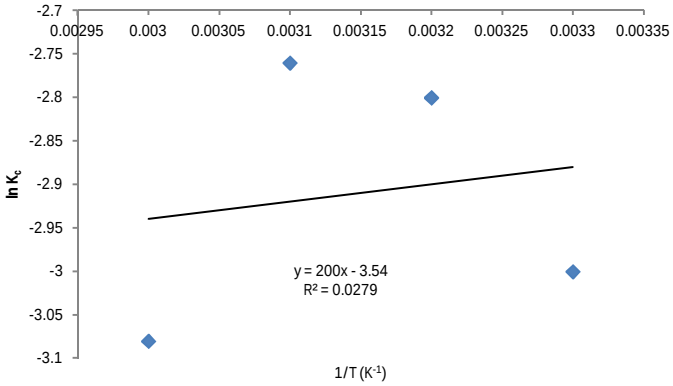


Figure 11: Van't Hoff's plot of 4-NA adsorption onto JAC.

The thermodynamic parameters (ΔG^o, ΔH^o and ΔS^o) for the adsorption of 4-NA onto JAC are listed in Table 5. The value of ΔH^o is practically zero. The entropy change of adsorption (ΔS^o) is negative indicating that the mobility of 4-NA on the surface of JAC is being more restricted in comparison with that in solution.[41]

Table 5: Thermodynamic parameters for 4-NA onto JAC.

ΔH^o (kJ/mol)	ΔS^o (kJ/mol/K)	T (K)	ΔG^o (kJ/mol)
-0.2	-0.029	303	8.69
		313	8.88
		323	9.17
		333	9.56

Conclusion

In this study, kaolinitic clay chemicaly activated using HNO_3 (AKC) and *Jatropha curcas* carbon chemically activated using NaOH (JAC) were investigated as possible adsorbents of 4-NA in aqueous solution. It was found that JAC is a potential and promising adsorbent of 4-NA while AKC is not. The adsorption of 4-NA by JAC was found to be strongly influenced by the initial concentration of 4-NA, contact time, solution pH, adsorbent dosage but not the temperature. The Langmuir, Freundlich, Temkin and Dubinin-Radushkevich models were used to examine the adsorption isotherms. The data could be fitted by the Freundlich equation much better than the other models. Pseudo-second order kinetic model provided the best fit for the experimental data and intra-particle diffusion was not involved in the adsorption process. The process is independent of temperature as there was no significant increase or decrease in the quantity of 4-NA adsorbed as the temperature increased.

References

[1] Gerald, B., Nitro Compounds, Aromatics in Ullmann's Encyclopedia of Industrial Chemistry", 7th Ed.; Wiley-VCH: Weinheim, 2005, doi:10.1002/14356007.a17_411.

[2] Williamson, K. L., Macroscale and Microscale Organic Experiments, Fourth Edition, Houghton-Mifflin, 2002, ISBN 0-618-19702-8.

[3] Bhunia, F.; Saha, N. C.; Kaviraj, A., *Ecotoxicology*. 2003, 12, 397-403.

[4] Oturan, M.A.; Peiroten, J.; Chartrin, P.; Acher, A. J., *Environ. Sci. Technol.,* 2000, 34, 3474-3479.

[5] Sun, J.H.; Sun, S.P.; Fan, M.H., *J. Hazard. Mater.,* 2007, 148, 172-177.

[6] Gautam, S.; Kamble, S.P.; Sawant, S.B., *Chem. Eng. J.,* 2005, 110, 129-137.

[7] Shen, L.R.; Yang, P.Z.; Chen, L.Y., *Tec. Water Tr. (Chinese)*, 1997, 23, 45-49.

[8] Saupe, A., *Chemosphere*, 1999, 39, 2325-2346.

[9] Panizza, M.; Cerisola, G., *Electrochim. Acta,* 2005, 51, 191-199.

[10] Pacheco, M. J.; Morao, A.; Lopes, A.; Cirıaco, L.; Goncalves, I., *Electrochim. Acta,* 2007, 53, 629-636.

[11] Saravanan, P.; Pakshirajan, K.; Saha, P., *Bioresour. Technol.,* 2008, 99, 205-209.

[12] Nazari, K.; Esmaeili, N.; Mahmoudi, A.; Rahimi, H.; Moosavi-Movahedi, A. A., *Enzyme Microb. Technol.,* 2007, 41, 226-233.

[13] Zheng, K.; Pan, B.C.; Zhang, Q.J., *Sep. Purif. Technol.,* 2007, 57, 250-256.

[14] Fatoki, O.S.; Ayanda, O.S.; Adekola, F.A.; Ximba, B.J., *Clean Soil Air Water*, 2008, 42, 472–479.

[15] Kunquan, Li.; Zheng, Z.; Jingwei, F.; Jibiao, Z.; Xingzhan, L.; Guohua, Z.; Xingfa, H., *J. Hazard. Mater.,* 2009, 166, 1180-1185

[16] El-Shahat, M.F.; Shehata, A.M.A., *International Journal of Emerging Technology and Advanced Engineering*, 2014, 4(1), 2250-2459

[17] Djebbar, M.; Djafri, F.; Bouchekara, M., *African Journal of Pure and Applied Chemistry*, 2012, 6(2), 15-25

[18] Atef, S. A.; Waleed, M., *Int'l. J. Phy.,* 2009, 4(4), 172-181.

[19] Adegoke, H.I.; Adekola, F.A., *Adv. in Natural and Applied Sciences*, 2010, 4(3), 293-298. ISSN 1995-0748.

[20] Hatem, A. A.; Maah, M. J.; Yahyar, R.; Radzi bin Abas, M., *Asian J. of Chem*. 2013, 25(17), 9575.

[21] Deer, W. A.; Howie, R. A.; Zussman, J.An introduction to the rock forming minerals, (1992), Second edition Harlow: Longman, ISBN 0-582-30094-0

[22] Pohl, W. L., Economic geology, principles and practice; metals, mineral, coal and hydrocarbons- Introduction to formation and sustainable exploitation of mineral deposits. Wiley Blackwell, 2011, 331. ISBN 978-1-4443-3662-7.

[23] Hadyn, H.M., Industrial application of kaolin, Georgia Kaolin Company, Elizabeth, New Jersey. 1955, Tenth National Conference on Clays and Clay Minerals.

[24] Janick, J.; Robert, E. P., The Encyclopaedia of Fruit & Nuts, 2008, CABI. 371–372. ISBN 978-0-85199-638-7.

[25] Achten, W. M. J.; Mathijs, E.; Verchot, L.; Singh, V.P.; Aerts, R.; Muys, B., *Biofuels, Bioproducts and Biorefining*, 2007 1(4); 283-291.

[26] Nahar, K.; Ozores-Hampton, M., Jatropha: An Alternative Substitute to Fossil Fuel (IFAS Publication Number HS1193), 2011, Gainesville: University of Florida, Institute of Food and Agricultural Sciences.

[27] Adebayo, T. A.; Ajayi, O., *Asian Transactions on Engineering*, 2011, 1(3); 2221-4267.

[28] Olokode, O.S.; Aiyedun, P.O., *Pacific J. Sci. and Technol.*, 2011, 12(2) 558-565.

[29] Tangjuank, S.; Insuk, N.; Tontrakoon, J.; Udeye, V., *World Academy of Sci. Eng. and Technol,* 2009, 52, 110-116.

[30] Karthikeyan, S.; Sakthivel, K., Kannan, C., *Rasayan J. Chem.,* 2011, 4(3), 519-532.

[31] Madejova, J., *Vibrational Spectroscopy*, 2003, 31; 1-10.

[32] Islam, M. S.; Rouf, M. A.; Fujimoto, S.; Minowa, T. Bangladesh *J., Sci. Ind. Res.,* 2012, 47(3), 257-264.

[33] Tongpoothorn, W.; Sriuttha, M.; Homchan, P.; Chanthai, S.; Ruangviriyachai, C., *Chem. Eng. Res. Des.,* 2011, 89(3), 335-340.

[34] Osman, D.; Erol A., *J. Hazard. Mater*., 2005, B120, 173–181.

[35] Tang, D.; Zheng, Z.; Lin, K.; Luan, J.; Zhang, J., *J. Hazard. Mater*., 2007, 143, 49–56.

[36] Uddin, M.; Islam, M.; Abedin, M., *ARPN Journal of Engineering and Applied Sciences,* 2007, 2, 11 - 16.

[37] Srivastava, V.C.; Swammy, M. M.; Mall, I.D.; Prasad, B.; Mishra, I.M., *Colloids Surf. A Physicochem Eng. Aspects*, 2006, 272, 89 – 104.

[38] Cotoruelo, L.M.; Marques, M.D.; Diaz, F.J.; Rodriguez-Mirasol, J.; Rodriguez, J.J.; Cordero, T., *Chem. Eng. J.,* 2012, 184, 176-183.

[39] Boparai, K. H.; Meera, J.; Denis, M. O., *J. Hazard. Mater.,* 2011, 186, 458–465.

[40] Atkins, P.; Julio de Paula, Physical chemistry 7th ed. New York, 2002, 987 – 994.

[41] Ai-min, L.; Hai-suo, W.; Quan-xing, Z.; Gen-cheng, Z.; Chao, L.; Zheng-hao, F.; Fu-qiang, L.; Jin-long, C., *Chinese J. Polymer Sci.,* 2004, 22(3), 259-269.